Environ Earth Sci (2016)75:810
DOI 10.1007/s12665-016-5603-8

ORIGINAL ARTICLE

Soil salinity distribution and its relationship with soil particle size in the lower reaches of Heihe River, Northwestern China

Yu Zhao[1,2,3] · Qi Feng[1] · Huaide Yang[1,2]

Received: 4 May 2015 / Accepted: 2 April 2016

Abstract Recognition of the vertical and spatial distribution characteristics of soil salinity and its influencing factors have become a prerequisite for formulating strategies for the utilization and sustainable development of soil resources. The changes and characteristics of the particle size distribution (PSD) and its relationship with soil salinity were studied using the combined methods of laser diffraction analysis, the textural triangle and fractal analysis in the lower reaches of Heihe River, Northwestern China. The soil salinity showed clear surface accumulation characteristics. Soil salinity profiles in the area were classified into four types: Equably distribution profiles, bottom accumulation profiles, surface accumulation profiles, and oscillation profiles. In the study area, moderate salinized soil, heavy salinized soil and saline soil accounted for 5.71, 25.71, and 42.87 %, respectively. It was shown that soil salinization in the lower reaches of Heihe River is severe. Soil salinity and its spatial distribution is mainly controlled by SO_4^{2-}, Cl^-, $Na^+ + K^+$, Mg^{2+}, and Ca^{2+}. The soil texture of the topsoil can be classified as sand, sandy loam, silt loam, and silt. The silt and sand occupied the majority of the PDS at different soil depths. There was a decrease in soil salinity and soil particle size with increasing soil depth. The fractal dimension of PSD ranged from 2.503 to 2.555, the higher the sand content, the lower the fractal dimension. A considerable linear relationship also exists between the fractal dimension and the contents of soil clay, silt, sand and the soil salinity. Results show that the soil texture features dominated the soil salinity distribution.

Keywords Soil salinity · Soil particle size distribution · Fractal dimension · Heihe River

Introduction

Soil salinization is a progressive process of soil degradation (Nawar et al. 2015), involving the accumulation of water soluble salts in the soil weathering layer. If this accumulation reaches 0.8 dS m^{-1}, salt toxicity occurs, which can damage agricultural production, economic welfare, and environmental health (Kotuby-Amacher et al. 1997; Flowers 2004; Fang et al. 2005; Rengasamy 2006). Soil salinization is one of the most important global environmental problems, especially in arid and semiarid regions (Chen et al. 2014). Information regarding the extent and magnitude of soil salinity is essential for the planning and implementation of effective soil reclamation programs (Abdelfattah et al. 2009).

Soil salinization and secondary salinization in arid and semi-arid regions are the result of natural conditions and human factors. Wang et al. (2008) pointed out that soil salinity increased gradually with decreasing of elevation from south to north in the Sangong River catchment in Xinjiang province, Northwest China. The results of this study showed that terrain elevation controlled the variability of surface soil salinity. According to Zhang et al. (2010), soil salinity differs from different physiognomy types as follows: the lower part of alluvial fan > the

✉ Qi Feng
qifeng@lzb.ac.cn

[1] Alashan Desert Eco-Hydrology Experimental Research Station, Cold and Arid Regions Environmental and Engineering Research Institute, Chinese Academy of Sciences, Lanzhou 730000, China

[2] University of Chinese Academy of Sciences, Beijing 100049, China

[3] Lanzhou University, Lanzhou 730000, China

Published online: 27 April 2016

middle of alluvial fan > the edge of the desert > the upper part of alluvial fan. This is related to the groundwater depth and degree of groundwater mineralization of the different physiognomy types. Fang et al. (2005) reported that salt content in Salic Fluvisols was significantly higher than in Gleyic Solonchaks in the Yellow River Delta. Zhang et al. (2011) revealed the influence mechanism of human activities on soil salinity, which confirms that oil exploitation and saline aquaculture contribute to salinization. However, the most important factors for soil salinization are strong evaporation and transpiration that cause the groundwater to rise above a critical depth (Gu et al. 2002). Evapotranspiration dries the upper soil relative to deeper layers, which create a potential for an upward flow of water into the root zone (Qadir et al. 2000).

Numerous studies have been conducted on soil salinization in the lower reaches of Heihe River. These studies have mainly focused on the regional distribution pattern of saline soils and the occurrence and dynamic characteristics of salinization (Zhong et al. 2002; Zhou et al. 2006; Liu et al. 2008; Gao et al. 2012; Chen et al. 2014). Studies have also been conducted into the relationship between soil salinity and plant growth (Yu et al. 2012), and the funnel distribution of soil salinity under the influence of groundwater chemistry (Zhang et al. 2004; Liu et al. 2005). However, few studies exist on the relationship between soil salinity and the composition of soil particle size.

Different soil textures and their combination in the soil vertical profile play an important role in governing the movements of soil moisture, nutrients, salinity and heat, as well as the secondary salinization of soil development (Yang and Yanful 2002). Soil textural analysis is a key component of any data set used for assessing soil quality and sustainability of agricultural management practices (Kettler et al. 2001). The application of fractal geometry has become a useful tool to describe the dynamics of soil degradation, for the purpose of explicitly quantifying the performance of soil systems. The soil particle size distribution (PSD) has an important influence on soil water movement, soil erosion and soil solute migrations (Montero 2005; Hu et al. 2011). Particle size distribution (PSD) is mainly used for soil classification and estimation of the related soil properties (Hillel 1980). Knowledge of the effects of PSD on soil salinity is essential for the complete understanding of the extent and causes of soil degradation. The fractal method can be used to describe the soil particle size distribution, pore size distribution and aggregate size distribution (Lipiec and Orellana 1998; Millan and Orellana 2001; Filgueira et al. 2006).

Quantitative study of the vertical distribution characteristics of soil salinity can accurately obtain information into regional salinization and potential salinization, which represents important information for use of agricultural production, management and environmental governance (Carter et al. 1993; Corwin et al. 2006). Therefore, we investigated the volume fractal dimension of soil particles and its relationship with soil salinity in order to reveal the characteristics and influencing factors of soil salinity in the lower reaches of Heihe River.

Materials and methods

Study area

The study area was located in the lower reaches of Heihe River and covers an area of 3.4×10^4 km^2 that extends between latitudes 40°42′–42°30′N and longitudes 99°30′–102°00′E (Guo et al. 2009). The region is surrounded by the Badan Jaran desert to the east, Mazong Mountain to the west, the Bei Mountain corridor to the south, and the Mongolia border to the north (Fig. 1). The region has an elevation between 890 and 1127 m above sea level (Wen et al. 2005). As a result of its location in the hinterland of the Asian continent, the study region has a continental climate that is extremely hot in summer and severely cold in winter. The average annual precipitation, evaporation, and temperature recorded from 1957 to 2001 at Ejina Meteorological Station was 38.5, 3599.4 mm, and 8.1 °C, respectively (Su et al. 2007). The sunshine hours was between 3325 and 3432 h. Relative humidity was between 32 and 36 % (Xi et al. 2009). Because of the scarce rainfall and high precipitation variability, no perennial runoff originates from the study area. The Heihe River is the only runoff flow through the area (He and Zhao 2006; Su et al. 2008). Because of the overexploitation of the water resources in the middle reaches of Heihe River, the discharge of water resources to the lower reaches have decreased significantly since the 1960s (Guo et al. 2009). The predominant soils are gypsum gray brown desert soil and grey brown desert soil in the lower reaches of Heihe River. Extreme arid climate conditions and poor soil conditions have limited the growth, development and distribution of plants in the study area. There are 11 species of vegetation in the lower reaches of Heihe River, which can be divided into two types: one is desert vegetation, the second is meadow vegetation and desert riparian forest. The former includes *Reaumuria soongorica* (Pall.) Maxim., *Nitrria shaerocarpa* Maxim., *Ephedra equisetina* Bunge, *Sarcozygium xanthoxylon* Bunge, *Sympegma regelii* Bunge, *Anabasis brevifolia* C.A.Mey., and *Calligonum mongolicunl* Turcz. The latter includes *Populus euphratica* Oliv., *Elaeagnus angustifolia* L., *Tamarix ramosissma* Ledeb., *Haloxylon ammodendron* (C.A.Mey.) Bunge, *Lycium ruthenicm* Murr., *Sophora alopecuroides* L., *Phragmites communis* (Cav.) Tein. Ex Steud.,

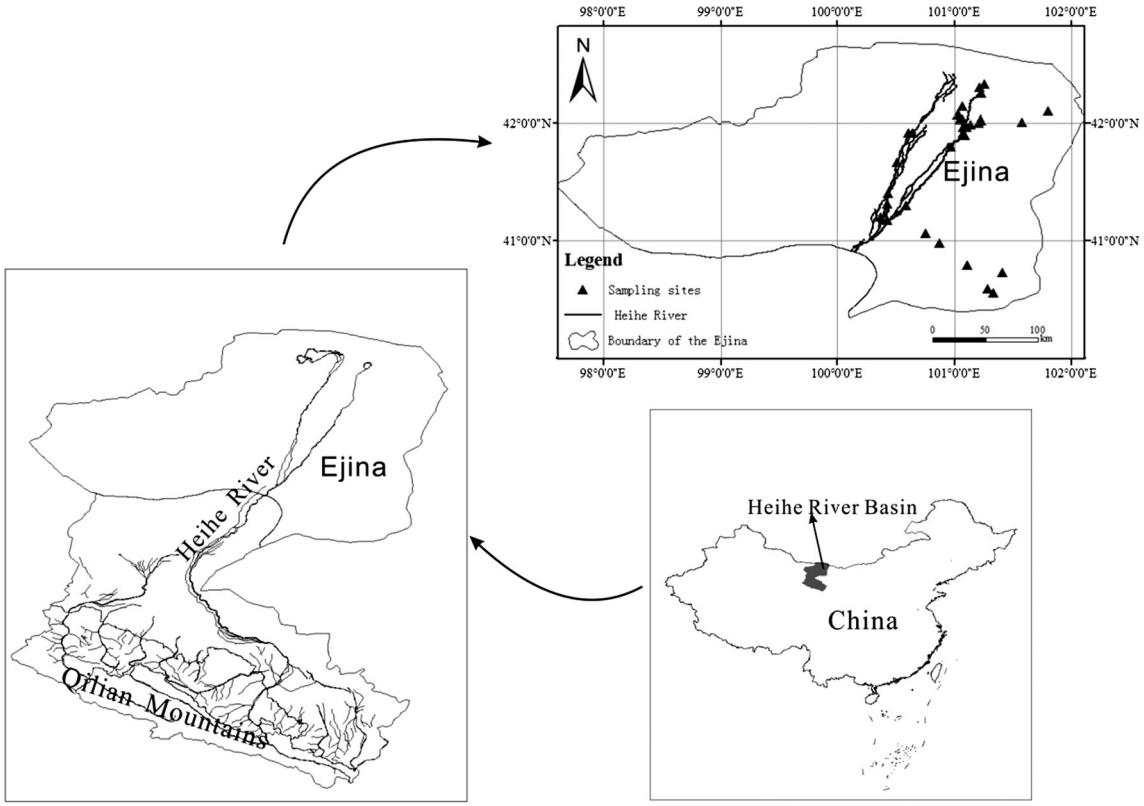

Fig. 1 Depiction of study area

Achnatherum splendens (Tein.) Nevski, and *Peganum harmala* L. (Feng et al. 2015).

Data collecting and processing

The sites for soil sampling were chosen along the river. A total of 35 soil sampling points were selected in the study area to reflect the vertical variation of soil salinity (Fig. 1). The soil was sampled in July 2011. Soil samples were taken from the 0–10, 10–20, 20–40, 40–60, 60–80 and 80–100 cm depth. Soil samples from the different depths were collected in triplicate.

Soil salinity measurement

Before the laboratory analysis, the soil samples were air-dried and passed through a 2 mm sieve to remove coarse fragments. Soil samples were used for the preparation of the 1:5 soil–water suspensions to detect the soil salinities (Yu and Wang 1988; Chi and Wang 2010). The following ions were measured (Yidana and Yidana 2010): carbonate (CO_3^{2-}) and bicarbonate (HCO_3^-) were titrated using the double indicator method; chloride (Cl^-) was measured by $AgNO_3$ liquor; sulfate (SO_4^{2-}), calcium (Ca^{2+}) and magnesium (Mg^{2+}) were measured with EDTA complexometry; sodium and potassium ($Na^+ + K^+$) were measured with subtraction method. Total dissolved salts (TDS) was calculated via the sum of anions and cations.

Laser diffraction analysis

As pretreatment of the soil samples, H_2O_2 (30 %, w/w) was first used to remove organic matter, then hexametaphosphate (NaHMP) was used to disperse the aggregates, and samples were then subjected to sonication for 30 s (Jin et al. 2013). In this study, we use a laser diffraction particle size analyzer (Malvern Instruments 2000, Malvern, England) to obtain the soil PSD. The range of particle sizes for this instrument was 0.02–2000 μm, which provides a continuous volume percentage of particle size.

Soil texture classification

In combination with the classification system of the United States Department of Agriculture, we make use of the soil texture automatic classification system (STAC) designed by Zhang Yili, to classify the soil texture in the study area. The theoretical basis of STAC is based on the fact that each point in a textural triangle represents a unique combination of clay, sand and silt content (Zhang et al. 2006).

Table 1 Statistical characteristics and K–S test of soil salinity at different soil depths

Soil depth (cm)	Mean (g/L)	SD	CV	Skewness	Kurtosis	K–S value	Sig.
0–10	41.12	66.89	1.63	2.47	6.49	1.69	0.007
10–20	18.48	33.04	1.79	3.40	13.43	1.81	0.003
20–40	6.84	6.64	0.97	1.15	0.29	1.19	0.115*
40–60	5.07	5.15	1.02	2.25	6.01	1.34	0.056*
60–80	4.34	4.21	0.97	1.53	1.15	1.49	0.024
80–100	3.85	4.30	1.12	2.61	7.09	1.50	0.023

SD standard deviation, *CV* coefficient of variation

* Correlation is significant at the 0.05 level (2-tailed)

Canonical correspondence analysis

To examine the relationship between the compositions of soil ions and soil salinity, canonical correspondence analysis (CCA) was applied using the CANOCO program V5.0 (Braak and Verdonschot 1995). The soil salt content was set as the research object, which is expressed by triangles, and the base ions were set as environmental variables expressed by arrows. Base ions included CO_3^{2-}, HCO_3^-, Cl^-, SO_4^{2-}, Ca^{2+}, Mg^{2+}, and $Na^+ + K^+$. A CCA ordination diagram can intuitively provide both the relationship between environmental variables and the relationship between the research object and environmental variables (Zhao et al. 2010). The CCA ordination diagrams show the best fitting environmental variables in the community composition and also indicate the proximate centers of species distribution along each of the environmental variables (Rogel et al. 2000).

There is an inverse relationship between the relevance and angle of two environmental variables, namely, the smaller the angle, the greater the correlation. The relationship between research objects and environmental variables is displayed by the angle between the research object and the environmental variables (the arrows), namely, the smaller the angle, the stranger the relationship.

The fractal analysis method for soil PSD

Fractal dimensions of PSD was estimated via the following equations (Tyler and Wheatcraft 1992):

$$W(\delta > d_i)/W_0 = 1 - (d_i/d_{\max})^{3-D} \quad (1)$$

$$\text{Or } (d_i/d_{\max})^{3-D} = W(\delta < d_i)/W_0 \quad (2)$$

where d_i is the mean diameter of soil particles of two sieves between d_i and d_{i+1}; $W(\delta > d_i)$ is the accumulative weight of soil particles with diameters greater than d_i; $W(\delta < d_i)$ is the accumulative weight of soil particles with diameters smaller than d_i; $d_{\max}$ is the largest diameter of soil particles; W_0 is the total weight of samples; and D is the fractal dimension.

Most previous studies have focused on the quality of the fractal dimension of soil PSD calculation. However, in the process of calculating the fractal dimension of soil mass, some hypotheses are needed. The hypotheses of the same density of soil particles with different particle size have been criticized by some scholars. In addition, using the traditional method to measure the distribution of soil particles is a large amount of work, and the results are more easily influenced by human factors (Wang et al. 2005). With the development and application of laser diffraction technique, the volume distribution of PSD can be obtained relatively easily and accurately.

The three-dimensional volume fractal dimension of PSD based on the distribution of soil particle was estimated using Eq. (3):

$$V(r < R_i)/V_T = (R_i/R_{\max})^{3-D_V} \quad (3)$$

where r is the particle size; R_i is the particle size of grade i in the particle size grading; $V(r < R_i)$ is the volume of soil particles with a diameter smaller than R_i; V_T is the volume of all of the soil particles; $R_{\max}$ is the maximum diameter of soil particles; and D_V is the volume fractal dimension (Yang et al. 1993; Martin and Montero 2002; Wang et al. 2005). Taking logarithms on both sides of Eq. (3), the D_V value can be derived from the slopes of the logarithmic linear regression equation.

Results and discussion

Distribution characteristics of soil salinity

The descriptive statistics and the results of the normal distribution test are shown in Table 1. The characteristic parameters of soil salinity showed distinct differences at different soil depths.

Average soil salinity decreased with the increase of soil depth in the study area (Table 1). There were clear soil salinity surface accumulation characteristics. A number of scholars have confirmed the ubiquity of the surface accumulation characteristics of soil salt (Zhang and Wang

2001; Rengasamy 2006; Cunningham et al. 2007; Chi and Wang 2010). This is due to the salt in the subsoil moving upward and accumulating in the topsoil as a function of evaporation (Yu et al. 2013). Liu et al. (2005) made use of empirical formula to calculate phreatic water evaporation and salt accumulation rate, which revealed that the surface soil salt accumulation had a negative exponential relation with groundwater depth.

If the Skewness and Kurtosis are close to 0 and 3, respectively, then the data are said to follow a normal distribution (Wu et al. 2014). The Skewness and Kurtosis are positive, and the TDS in different soil depths all exhibited non-normal distribution (Table 1).

The coefficients of variation (CV) represent the dispersion of the soil salinity distribution. When CV < 10 %, the soil salinity manifests low-variability, when 10 % < CV < 100 %, the soil salinity demonstrates medium-variability, and when CV > 100 %, the soil salinity is considered highly variable (Wang et al. 2001). As shown in Table 1, the high value for CV in the present analysis indicated a high variability of soil salinity of 0–10, 10–20, 40–60, and 80–100 cm soil depth. The CV values of the soil salinity demonstrated medium-variability at 20–40 and 60–80 cm soil depth.

The large SD and CV (mostly >1) indicate a large variability in the soil salinity in the study area. This agrees with the study of Jia et al. (2008), conducted in the lower reaches of Heihe River in 2006, which concluded that the CV of soil salinity was 1.65. The reasons for the strong variation of soil salinity in the study are the changes of hydrogeological conditions, soil structure, landscape type, landform, rainfall and evaporation in different regions in the lower reaches of Heihe River (Wang et al. 2009).

The one-sample Kolmogorov–Smirnov Test indicated that soil salinity at 20–40 and 40–60 cm soil depth followed a normal distribution ($K–S_{Sig > 0.05}$), and the soil salinity at others depths followed non-normal distributions.

The distribution characteristics of soil salinity profiles are shown in Fig. 2. Based on the analysis, soil salinity profiles in the area are classified into four types: oscillation profiles, equably distribution profiles, bottom accumulation profiles, and surface accumulation profiles. Equably distribution profiles were featured with the lowest and equal distribution of salinity. Bottom accumulation profiles distributed in the East Juyan Lake. Surface accumulation profiles were mainly distributed in the downstream of the East River and Gobi area.

There was significant positive correlation between the soil salinity at different soil depths, with the correlation coefficients ranging from 0.168 to 0.809 (Table 2).

The correlation coefficient of soil salinity was 0.465, 0.364, 0.647, 0.762, and 0.809 for soil depths between 0–10 and 10–20 cm, between 10–20 and 20–40 cm, between 20–40 and 40–60 cm, between 40–60 and 60–80 cm, and between 60–80 and 80–100 cm, respectively. This shows that the soil salinity in a specific soil layer is determined by the soil salinity of the adjacent subsoil.

The Eqs. 4a, 4b, 4c, 4d, 4e, 4f present the relationship between soil salinity of different soil depths by multiple linear regression. Analysis of variance and the significance test of regression coefficient of the established equations revealed that the regression equations are significant.

$$\begin{aligned} TDS_{0-10} &= 1.879TDS_{10-20} + 0.671TDS_{20-40} \\ &\quad + 0.341TDS_{40-60} - 1.000TDS_{60-80} \\ &\quad + 0.722TDS_{80-100} + 1.000; \\ R^2 &= 0.904, \quad F = 52.879, \ \text{Sig} = 0.000 \end{aligned} \tag{4a}$$

$$\begin{aligned} TDS_{10-20} &= 0.462TDS_{0-10} - 0.270TDS_{20-40} \\ &\quad - 0.095TDS_{40-60} + 0.820TDS_{60-80} \\ &\quad - 0.241TDS_{80-100} - 0.544; \\ R^2 &= 0.903, \quad F = 52.253, \ \text{Sig} = 0.000 \end{aligned} \tag{4b}$$

$$\begin{aligned} TDS_{20-40} &= 0.035TDS_{0-10} - 0.057TDS_{10-20} \\ &\quad + 0.589TDS_{40-60} + 0.742TDS_{60-80} \\ &\quad - 0.512TDS_{80-100} + 2.404; \\ R^2 &= 0.488, \ F = 5.334, \ \text{Sig} = 0.001 \end{aligned} \tag{4c}$$

$$\begin{aligned} TDS_{40-60} &= 0.007TDS_{0-10} - 0.008TDS_{10-20} \\ &\quad + 0.242TDS_{20-40} + 0.590TDS_{60-80} \\ &\quad + 0.108TDS_{80-100} - 0.183; \\ R^2 &= 0.648, \ F = 10.292, \ \text{Sig} = 0.000 \end{aligned} \tag{4d}$$

$$\begin{aligned} TDS_{60-80} &= -0.008TDS_{0-10} + 0.028TDS_{10-20} \\ &\quad + 0.120TDS_{20-40} + 0.232TDS_{40-60} \\ &\quad + 0.518TDS_{80-100} + 0.193; \\ R^2 &= 0.795, \ F = 21.752, \ \text{Sig} = 0.000 \end{aligned} \tag{4e}$$

$$\begin{aligned} TDS_{80-100} &= 0.010TDS_{0-10} - 0.013TDS_{10-20} \\ &\quad - 0.137TDS_{20-40} + 0.070TDS_{40-60} \\ &\quad + 0.858TDS_{60-80} + 0.599; \\ R^2 &= 0.675, \ F = 11.62, \ \text{Sig} = 0.000 \end{aligned} \tag{4f}$$

where the subscripts of 0–10, 10–20, 20–40, 40–60, 60–80, and 80–100 represents soil depths of 0–10, 10–20, 20–40, 40–60, 60–80, and 80–100 cm, respectively.

The distribution characteristics of anions and cations in the soil profile are shown in Fig. 3. SO_4^{2-} is the major anion in the study area, which occupies the absolute advantage in the total anions content in each soil depth with a percentage ≥65 %. Cl^- is another important anion in the study area, at between 20 and 30 % of the total anions content. The content of CO_3^{2-} was almost the same in each soil layer. The content of SO_4^{2-}, Cl^- and HCO_3^- decreased with the increase of soil depth. The CV values of

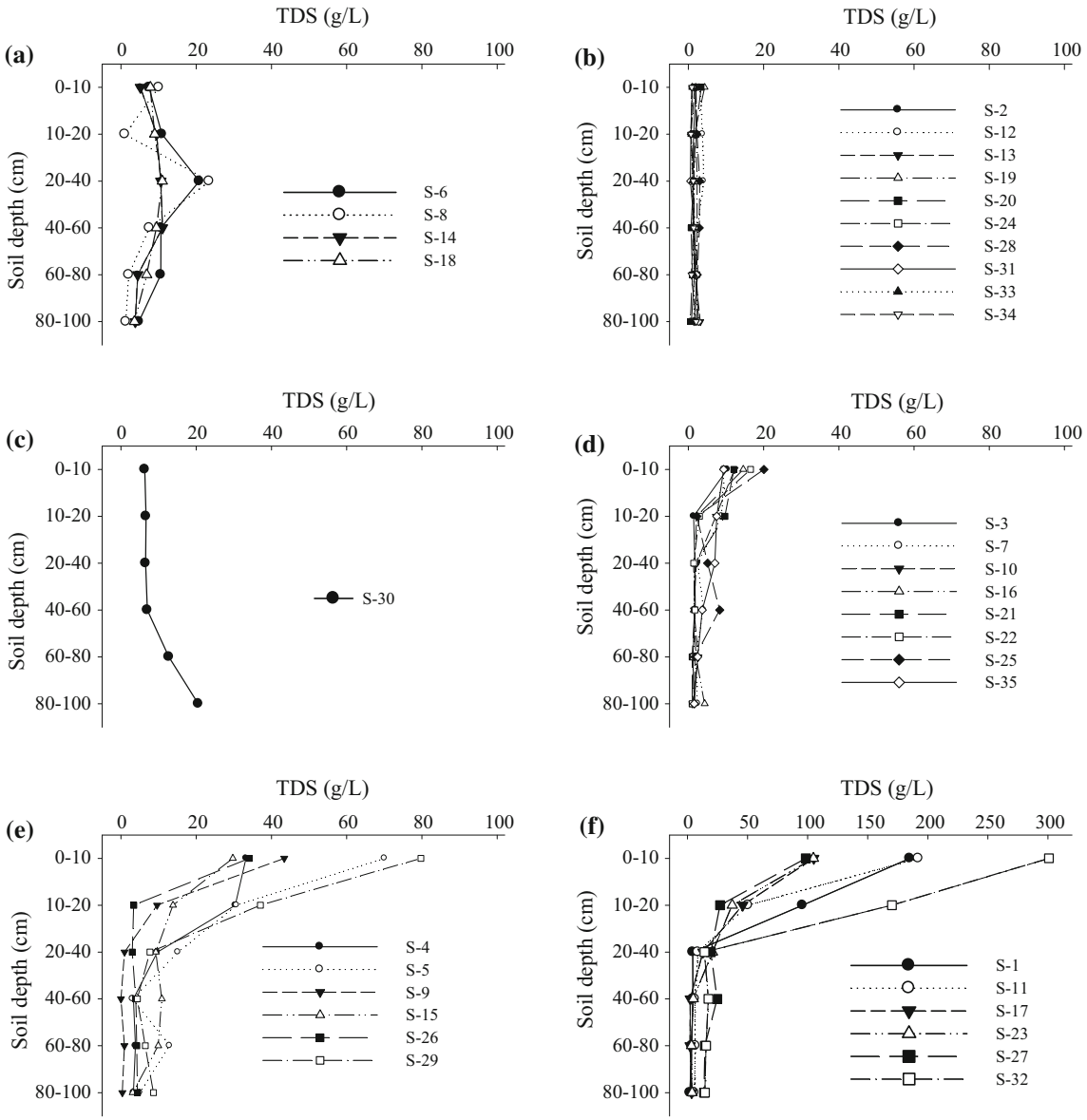

Fig. 2 Classification of salinity profiles in the lower reaches of the Heihe River (**a** oscillation profiles; **b** equably distribution profiles; **c** bottom accumulation profiles; **d–f** surface accumulation profiles)

Table 2 Relationships of soil salinity between different soil depths via the Pearson correlation analysis

Soil depth (cm)	0–10	10–20	20–40	40–60	60–80	80–100
0–10	1					
10–20	0.465**	1				
20–40	0.395*	0.364*	1			
40–60	0.355*	0.168	0.647**	1		
60–80	0.431**	0.256	0.593**	0.762**	1	
80–100	0.348*	0.168	0.371*	0.612**	0.809**	1

* Correlation is significant at the 0.05 level (2-tailed)

** Correlation is significant at the 0.01 level (2-tailed)

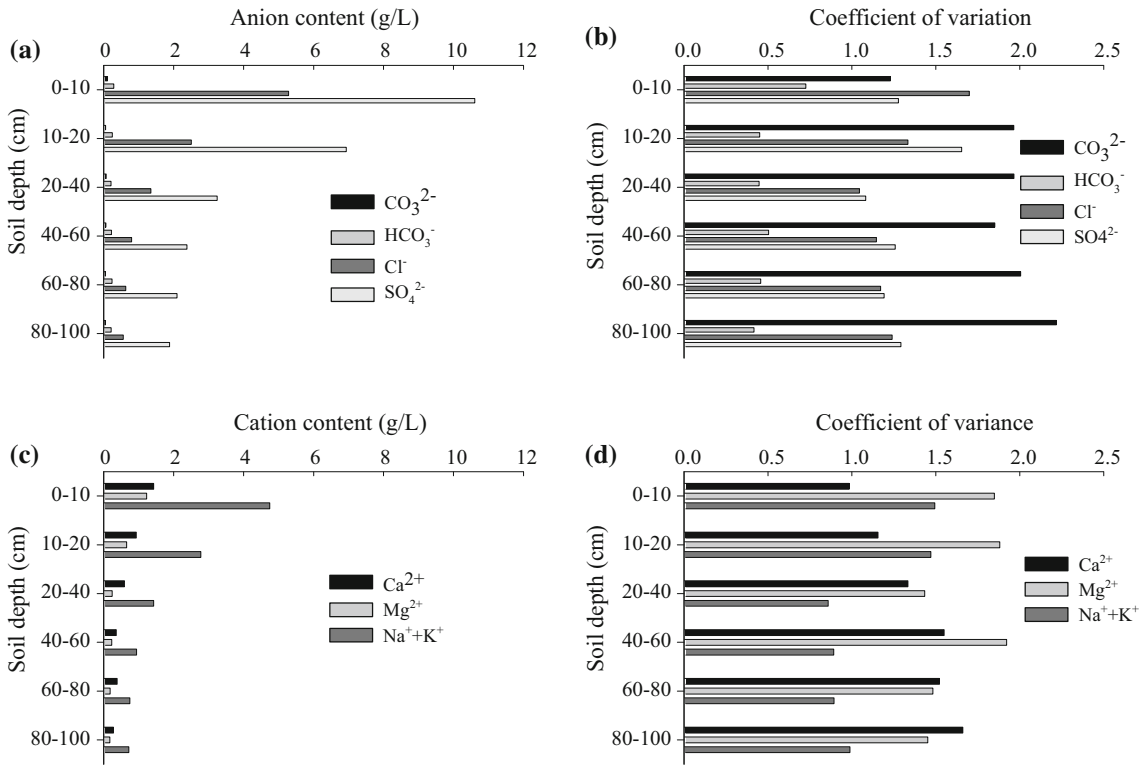

Fig. 3 Vertical variation of anions and cations in the soil profile

SO_4^{2-} and CO_3^{2-} exhibited an inverse "S" shaped curve with the increase of soil depth. In addition, the CV values of HCO_3^- and Cl^- decreased gradually and tended towards stability with the increase of soil depth. SO_4^{2-}, Cl^- and CO_3^{2-} exhibited a high-variability, with a CV greater than 100 %. HCO_3^- exhibited medium-variability, with a CV between 10 and 100 %. $Na^+ + K^+$ is the major cations in the study area, with the percentage of total cations content ranging from 57 to 64 %. The content of $Na^+ + K^+$, Ca^{2+} and Mg^{2+} decreased with the increase of soil depth. The CV value of $Na^+ + K^+$ decreased gradually and tended towards stability with increased soil depth. Variation of Mg^{2+} displayed an "S" shaped curve with increased soil depth. In addition, variation of Ca^{2+} increased with increased soil depth. Ca^{2+} and Mg^{2+} exhibited high-variability, with CV values greater than 100 %. $Na^+ + K^+$ at 20–40, 40–60, 60–80, and 80–100 cm soil depths exhibited medium-variability, with the CV values ranging from 10 to 100 %. The distribution characteristics of anions and cations in the soil vertical profile is consistent with the results of Zhang et al. (2004). Meanwhile, Zhou et al. (2006) reported that the concentrations of soluble ions and soil salinity have a tendency to decrease with the increasing soil depth in the lower reaches of Heihe River.

The regression equations between soil depth and soil salinity and the ionic concentration are shown in Table 3. All regression equations reached the 0.05 significance level, which revealed that all regression equations are significant.

Vertical variation law, seasonal variation characteristics, and horizontal variation regularity are all important aspects to characterize soil salinization characteristic. Figure 4a shows the variety patterns of soil salinity in different seasons (the spring of 2001 and the summer of 2011) in the lower reaches of Heihe River. Figure 4b–d show the seasonal variation characteristic of soil salinity in the Qaidam Basin (Jia et al. 2002), Keriya Oasis (Halmurat et al. 2008), and Ebinur Lake (Deng et al. 2013), respectively. Characteristics of climate and soil salinization are similar among the lower reaches of Heihe River, Qaidam Basin, Keriya Oasis, and Ebinur Lake, which embodied in few precipitation and strong evaporation, surface accumulation of soil salt, and severe salinization. Soil salt movement showed obvious seasonal variation, and salt content in spring was higher than that in summer in Qaidam Basin, and Keriya Oasis. Salt content in spring of 2001 was less than that in summer of 2011 in the lower reaches of Heihe River (Fig. 4a). From this we can know that the salt content in summer of 2001 was less than that in summer of 2011 in the studied area, which indicated that the soil salinity showed an increasing trend in the lower reaches of Heihe River over the past 10 years. The

Table 3 Relationship between soil depth and soil ions and the salinity

Item	Regression equation (Y = content/g L^{-1}; X = depth/cm)	R^2	F	Sig.
TDS-depth	$Y_{TDS} = 163.08\ X^{-0.862}$	0.975	158.124	0.000
CO_3^{2-}-depth	$Y_{CO_3^{2-}} = 0.018\ X^{-0.336}$	0.761	12.714	0.023
HCO_3^--depth	$Y_{HCO_3^-} = 0.065\ X^{-0.268}$	0.789	14.975	0.018
Cl^--depth	$Y_{Cl^-} = 4.032\ X^{-0.979}$	0.994	663.515	0.000
SO_4^{2-}-depth	$Y_{SO_4^{2-}} = 7.685\ X^{-0.855}$	0.963	105.517	0.001
Ca^{2+}-depth	$Y_{Ca^{2+}} = 0.584\ X^{-0.670}$	0.978	174.981	0.000
Mg^{2+}-depth	$Y_{Mg^{2+}} = 0.839\ X^{-0.909}$	0.944	67.714	0.001
$Na^+ + K^+$-depth	$Y_{Na^+ + K^+} = 3.990\ X^{-0.929}$	0.981	205.673	0.000

In the regression equations, 5, 15, 30, 50, 70, and 90 cm represents the soil depth of 0–10, 10–20, 20–40, 40–60, 60–80, and 80–100 cm, respectively

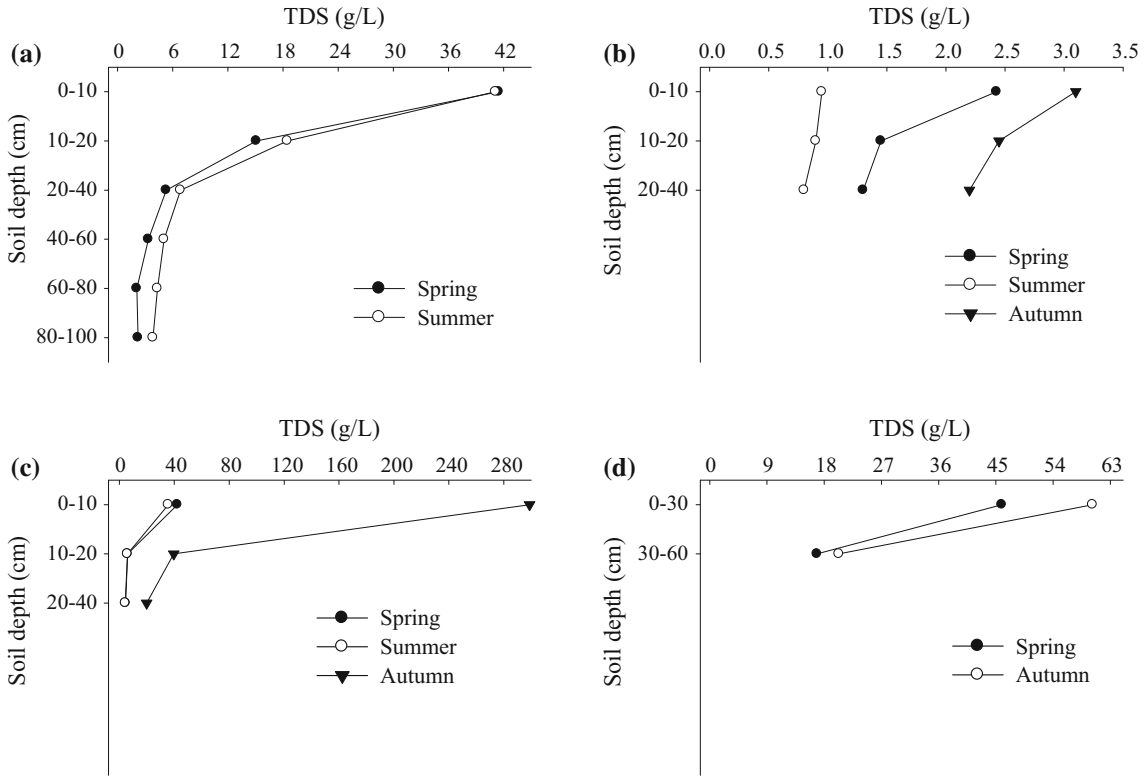

Fig. 4 Variety patterns of soil salinity in different seasons (**a** the lower reaches of Heihe River; **b** Qaidam Basin; **c** Keriya Oasis; **d** Ebinur Lake)

reason for seasonal changing characteristics of salt movement is the duel rule of leaching and evaporation in saline areas of north China. Soil salt accumulates under the action of evaporation in spring and autumn. Soil salt desalinate by eluviation in summer. Soil salt is relatively stable in winter (Jia et al. 2002).

The predominant salt type is important because of the effect of individual ions on the soil and possibility of toxicity in plants (Cebas-Csic et al. 1997). Soil classification by the Professional Committee of saline soil of Soil Science Society of China is: when $Cl^-/SO_4^{2-} > 2$, soil belongs to chloride; when $1 \le Cl^-/SO_4^{2-} < 2$, soil belongs to sulfate–chloride; when $0.2 \le Cl^-/SO_4^{2-} < 1$, soil belongs to chloride–sulfate; when $Cl^-/SO_4^{2-} < 0.2$, soil belongs to sulfate. The main salt types are chloride–sulfate and sulfate in different soil depths in the study area (Table 4). Zhu et al. (2009) made use of piper plot of chemical analysis to show that the majority of groundwater samples were of sulfate type in the lower reaches of Heihe River. The result indicates that soil salinity is related to groundwater salinity. Table 4 showed the classification standard of soil salinization under the salt types of chloride,

Table 4 Salt type and soil salinization status in the lower reaches of Heihe River

Soil depth (cm)	Chloride $2 \leq Cl^-/SO4^{2-}$ (%)	Sulfate–chloride $1 \leq Cl^-/SO4^{2-} < 2$ (%)	Chloride–sulfate $0.2 \leq Cl^-/SO4^{2-} < 1$ (%)	Sulfate $Cl^-/SO4^{2-} < 0.2$ (%)
0–10	2.86	5.71	82.86	8.57
10–20	0.00	8.57	77.14	14.29
20–40	0.00	2.85	82.86	14.29
40–60	0.00	8.57	62.86	28.57
60–80	2.86	0.00	80.00	17.14
80–100	0.00	5.72	71.43	22.85
Grading of soil salinization	Chloride	Sulfate–chloride	Chloride–sulfate	Sulfate
Non saline				
Criteria	$TDS_{0-10} < 1.5$	$TDS_{0-10} < 2.0$	$TDS_{0-10} < 2.5$	$TDS_{0-10} < 3.0$
Value			20.00 %	
Light salinized				
Criteria	$1.5 \leq TDS_{0-10} < 3.0$	$2.0 \leq TDS_{0-10} < 3.0$	$2.5 \leq TDS_{0-10} < 4.0$	$3.0 \leq TDS_{0-10} < 6.0$
Value			5.71 %	
Moderate salinized				
Criteria	$3.0 \leq TDS_{0-10} < 5.0$	$3.0 \leq TDS_{0-10} < 6.0$	$4.0 \leq TDS_{0-10} < 7.0$	$6.0 \leq TDS_{0-10} < 10.0$
Value		2.85 %	2.86 %	
Heavy salinized				
Criteria	$5.0 \leq TDS_{0-10} < 8.0$	$6.0 \leq TDS_{0-10} < 10.0$	$7.0 \leq TDS_{0-10} < 12.0$	$10.0 \leq TDS_{0-10} < 20.0$
Value		7.86 %	17.14 %	5.71 %
Salinized soil				
Criteria	$TDS_{0-10} \geq 8.0$	$TDS_{0-10} \geq 10.0$	$TDS_{0-10} \geq 12.0$	$TDS_{0-10} \geq 20.0$
Value	2.86 %		37.15 %	2.86 %

Percentage during the table is the ratio of the corresponding sampling points to the total sample points

TDS_{0-10} Total amount of salt in the soil depth of 0–10 cm (g/L)

sulfate–chloride, chloride–sulfate, and sulfate. In the study area, moderate salinized soil, heavy salinized soil and saline soil accounted for 5.71, 25.71, and 42.87 %, respectively. Results show that soil salinization in the lower reaches of Heihe River is severe.

The correlation between soil salinity content and salt base ions in the lower reaches of Heihe River are shown in Table 5. The correlation coefficient between total soil salinity and SO_4^{2-} is the maximum at different soil depth. There are significant positive correlation between soil salinity and the content of $Cl^-/SO_4^{2-}/Ca^{2+}/Mg^{2+}/Na^+ + K^+$ with the vertical soil profile. In addition, a significant positive correlation was found between soil salinity and content of CO_3^{2-}/HCO_3^- in the 0–10 cm soil depth. However, at other soil depths, soil salinity was not related to the content of CO_3^{2-}/HCO_3^-.

Two-dimensional ordination diagrams for canonical correspondence analysis of salts at various soil depths are shown in Fig. 5. Cl^- is highly positively correlated with $Na^+ + K^+$ at different soil depths. Additionally, SO_4^{2-} is highly correlated with $Na^+ + K^+$ at different soil depths, with a correlation coefficient less than the correlation coefficient for Cl^-, and $Na^+ + K^+$ (Fig. 5).

Based on the angle from TDS to SO_4^{2-}, Cl^-, $Na^+ + K^+$, Mg^{2+}, and Ca^{2+}, we know that the spatial variability of soil salinity is similar to the environmental factors SO_4^{2-}, Cl^-, $Na^+ + K^+$, Mg^{2+}, and Ca^{2+}. Therefore, the soil salinity and its spatial distribution is mainly controlled by SO_4^{2-}, Cl^-, $Na^+ + K^+$, Mg^{2+}, and Ca^{2+}. The angles from TDS to CO_3^{2-} and HCO_3^- are larger at soil depths of 0–10, 10–20, 20–40, 40–60, 60–80, and 80–100 cm, which indicates that CO_3^{2-} and HCO_3^- have less effect on the soil salinity.

The spatial distribution maps of soil salinity and soil ions in the soil depth of 0–10 cm were achieved using Kriging interpolation (Fig. 6). Before the spatial interpolation analysis, the data was logarithmically transformed. After transformation, all data sets followed the normal distribution. Figure 6 shows that the spatial distribution characteristic of soil base ions is consistent with soil salinity. Soil ions and soil salinity were scatted in the study area. Overall, low soil ions and soil salinity were

Table 5 Correlative matrices of ions and soil salinity at different soil depths

Soil depth (cm)	Value							
	CO_3^{2-}	HCO_3^-	Cl^-	SO_4^{2-}	Ca^{2+}	Mg^{2+}	$Na^+ + K^+$	TDS
0–10								
CO_3^{2-}	1							
HCO_3^-	−0.11	1						
Cl^-	0.38*	0.21	1					
SO_4^{2-}	0.43**	0.50**	0.70**	1				
Ca^{2+}	0.71**	0.02	0.64**	0.63**	1			
Mg^{2+}	0.22	0.57**	0.56**	0.93**	0.36*	1		
$Na^+ + K^+$	0.42*	0.29	0.98**	0.78**	0.66**	0.64**	1	
TDS	0.38*	0.55**	0.57**	0.97**	0.53*	0.95**	0.67**	1
10–20								
CO_3^{2-}	1							
HCO_3^-	−0.25	1						
Cl^-	0.25	0.19	1					
SO_4^{2-}	0.20	0.34*	0.64**	1				
Ca^{2+}	0.20	0.19	0.78**	0.74**	1			
Mg^{2+}	0.03	0.35*	0.66**	0.93**	0.66**	1		
$Na^+ + K^+$	0.34*	0.30	0.79**	0.94**	0.74**	0.84**	1	
TDS	0.24	0.33	0.79**	0.98**	0.81**	0.92**	0.98**	1
20–40								
CO_3^{2-}	1							
HCO_3^-	−0.42*	1						
Cl^-	0.24	−0.22	1					
SO_4^{2-}	026	−0.17	0.67**	1				
Ca^{2+}	0.25	−0.24	0.55**	0.94**	1			
Mg^{2+}	0.20	−0.05	0.61**	0.79**	0.60**	1		
$Na^+ + K^+$	0.32	−0.20	0.94**	0.77**	0.64**	0.57**	1	
TDS	0.30	−0.20	0.84**	0.97**	0.88**	0.77**	0.90**	1
40–60								
CO_3^{2-}	1							
HCO_3^-	−0.17	1						
Cl^-	−0.20	−0.02	1					
SO_4^{2-}	−0.18	−0.15	0.73**	1				
Ca^{2+}	−0.12	−0.31	0.40*	0.77**	1			
Mg^{2+}	−0.18	−0.03	0.70**	0.81**	0.30	1		
$Na^+ + K^+$	−0.08	0.31	0.92**	0.81**	0.51**	0.64**	1	
TDS	−0.16	−0.10	0.84**	0.98**	0.72**	0.81**	0.90**	1
60–80								
CO_3^{2-}	1							
HCO_3^-	−0.30	1						
Cl^-	−0.23	0.00	1					
SO_4^{2-}	−0.27	−0.72	0.60**	1				
Ca^{2+}	−0.19	−0.22	0.31	0.87**	1			
Mg^{2+}	−0.25	0.38	0.79**	0.71**	0.35*	1		
$Na^+ + K^+$	−0.18	0.10	0.86**	0.78**	0.47**	0.69**	1	
TDS	−0.26	−0.35	0.75**	0.98**	0.79**	0.77**	0.88**	1
80–100								
CO_3^{2-}	1							
HCO_3^-	−0.20	1						

Table 5 continued

Soil depth (cm)	Value							
	CO_3^{2-}	HCO_3^-	Cl^-	SO_4^{2-}	Ca^{2+}	Mg^{2+}	$Na^+ + K^+$	TDS
Cl^-	−0.20	0.03	1					
SO_4^{2-}	−0.21	−0.13	0.84**	1				
Ca^{2+}	−0.09	−0.24	0.62**	0.86**	1			
Mg^{2+}	−0.24	−0.07	0.91**	0.89**	0.61**	1		
$Na^+ + K^+$	−0.18	0.06	0.91**	0.91**	0.62**	0.88**	1	
TDS	−0.19	−0.07	0.90**	0.99**	0.82**	0.91**	0.94**	1

* Correlation is significant at the 0.05 level (2-tailed)

** Correlation is significant at the 0.01 level (2-tailed)

distributed in the Ejina Oasis and along the river bed, and high soils ions and salinity were distributed in West Juyan Lake and Gurinai area. Wen et al. (2005) and Zhu et al. (2009) investigated the hydrogeochemical process in the groundwater environment of the lower reaches of Heihe River, the results indicate that groundwater in the area is brackish and the rock weathering and evaporation deposition as well as dissolution of minerals, such as halite, gypsum, dolomite, silicate and mirabilite in the sediments are the dominant processes that determine the major ionic composition in the study area. Evapotranspiration made chemical components concentrated in the groundwater and resulted in the occurrence of salt crust in the center of Ejina basin. The salt ion contents and soil salinity did not show a trend of increasing along the river, which is not entirely consistent with the increase of groundwater salinity along the river. This may be caused by the salt absorption by plants, which occurred in the patch shaped green space in the lower reaches of Heihe River in both sides and Ejina oasis (Yi et al. 2007).

Soil particle size distributions and their relationship with soil salinity

The PDS was divided into 3 levels; namely, clay (0–2 μm), silt (2–50 μm) and sand (50–2000 μm). Soil texture was distinguished by the mass of each soil grade. Table 6 presents the distribution of soil particle sizes at different soil depths in the lower reaches of Heihe River.

The soil texture of topsoil can be classified as sand, sandy loam, silt loam, and silt. At 0–10 cm soil depth, sand was the most common category (58.49 %) followed by silt (35.94 %), and clay (4.57 %). The silt and sand occupied the majority of the soil particle distribution at the other measured soil depths. The silt content ranged from 28.37 to 37.61 % at the other measured soil depths, and sand content ranged from 58.49 to 68.03 %. Figure 7 shows that there is a positive relationship between clay and silt content, and there is a strong negative relationship between clay and sand content. This result is consistent with the results of Acosta et al. (2009), who showed a similar relationship between clay content and silt/sand content in Xinjiang of China.

Tables 1 and 6 together shows that the soil salinity and soil particle size decreased with increasing soil depth. The relationship between soil salinity and soil particle size is consistent with the relationship between soil metal content and soil particle size. Al-Rajahi et al. (1996) and Ljung et al. (2006) showed that the concentration of metals in soil increases with decreasing soil particle size. This is because fine particles have a high specific area that retains high amounts of metals (Acosta et al. 2009).

Table 7 contains the fractal dimension of PSD found when Eq. (3) was applied to each soil data set. Fractal dimensions of PSD (D_V) varied between the vertical profiles of soil at different depths, ranging from 2.503 to 2.555. Fu et al. (2009) similarly showed that the fractal dimension of PSD distribution ranged from 2.06 to 2.66 along an altitudinal gradient in the Alxa Rangeland of western Inner Mongolia.

The fractal dimensions of soil clay, silt and sand were calculated, and they were denoted D_{Clay}, D_{Silt}, and D_{Sand}, respectively. The value of D_{Silt} ranged from 2.305 to 2.705 and the value of D_{Sand} ranged from 2.512 to 2.609. The relationships between D_{Clay}, D_{Silt}, and D_{Sand} are $D_{\text{Clay}} < D_{\text{Silt}} < D_{\text{Sand}}$ (Table 7). The fractal dimensions of soil particles increased with finer soil textures. The fractal dimension of soil sand was significantly affected by silt contents. The lowest value of D_{Sand} (2.512) corresponded to the soil depth of 80–100 cm which had lowest clay and silt contents (31.97 %), but highest sand content (68.03 %), while the highest D_{Sand} (2.609) was found at 0–10 cm soil depth, which had highest clay and silt contents (41.45 %), but lowest sand content (58.49 %). The results indicate that the removal of fine particles (clay and silt) resulted in decreased D_{Sand} value (Su et al. 2004). Huang and Zhan (2002) similarly showed that the fractal dimension of PSD decreased with increasing sand content but increased with increasing clay content.

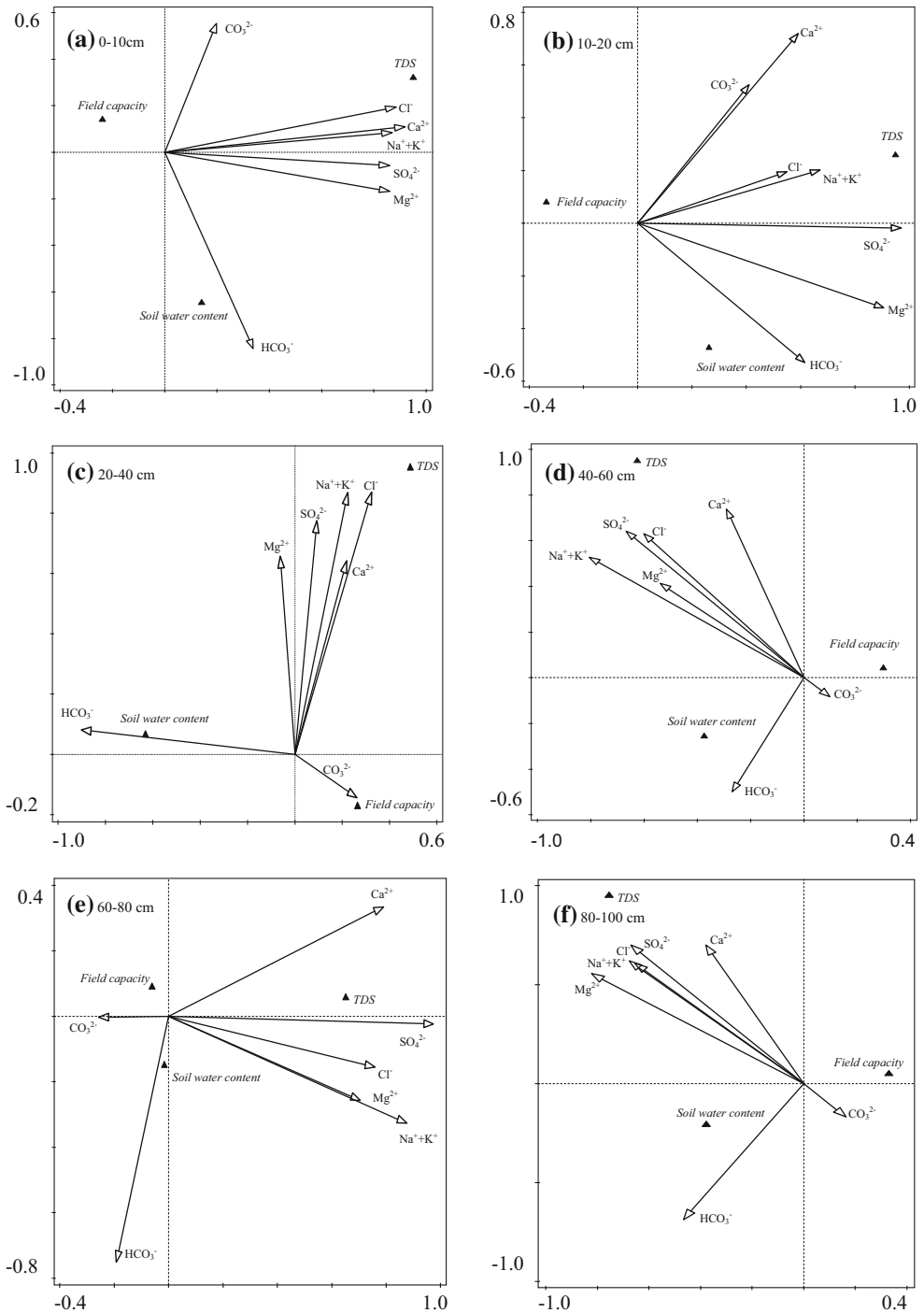

Fig. 5 Two-dimensional ordination diagram for canonical correspondence analysis of salts at various soil depths

A correlation analysis was carried out on the content of soil ions/salinity and soil PSD to evaluate the relationship between soil ions/salinity and soil texture at the different soil depths (Table 8). Comparing the content of soil ions/salinity and sand, all elements except CO_3^{2-} showed a negative correlation at different soil depths, although there was a great variation in the strength of this relationship. Positive correlations were found between content of soil ions/salinity and clay/silt, except for CO_3^{2-} and Ca^{2+}. It was shown that soil texture does not affect the content of CO_3^{2-} and Ca^{2+}.

A simple linear regression analysis was applied to establish the relationship between *D* and clay, silt, and clay contents, and soil salinity (Fig. 8). Figure 8 shows that the

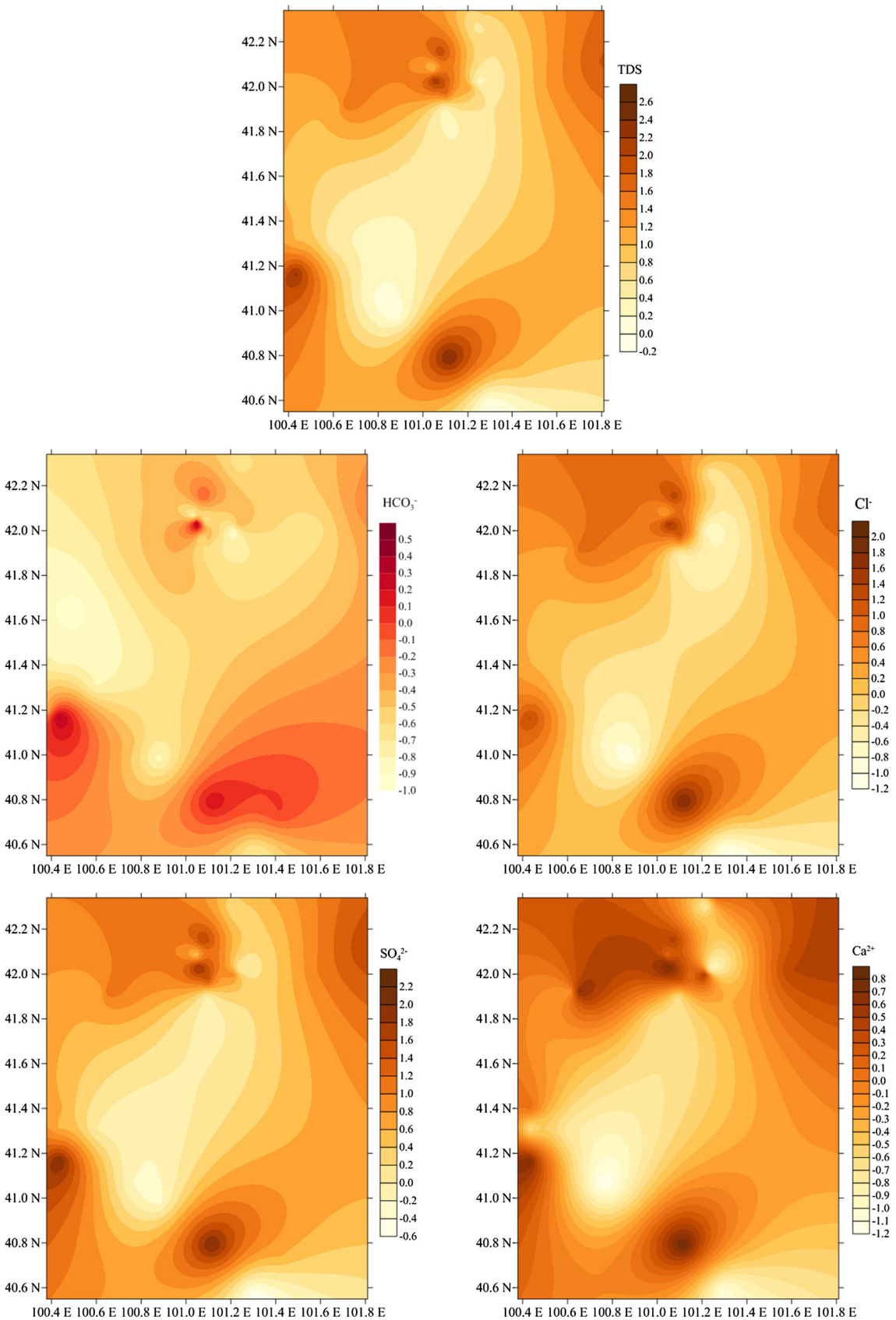

Fig. 6 Spatial distribution of soil salinity and soil ions at the 0–10 cm soil depth

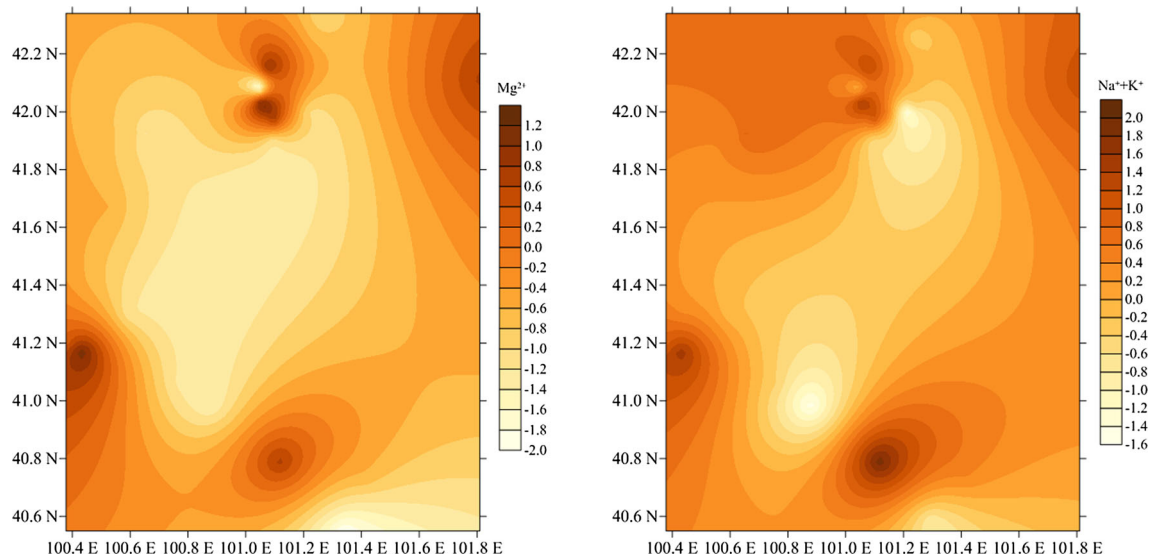

Fig. 6 continued

Table 6 Soil particle size distribution in the soil profile

Soil depth (cm)	Soil particle content (%)			Soil texture
	<2 μm Clay	2–50 μm Silt	50–2000 μm Sand	
0–10	4.57	36.94	58.49	Sand, sandy loam, silt loam, silt
10–20	4.72	37.61	59.47	Sand, sandy loam, silt loam, silt
20–40	3.52	32.05	64.43	Sand, loamy sand, sandy loam, silt loam, silt
40–60	4.31	34.28	61.41	Sand, loamy sand, sandy loam, silt loam, silt
60–80	4.00	32.24	63.76	Sand, loamy sand, sandy loam, silt loam, silt
80–100	3.60	28.37	68.03	Sand, loamy sand, sandy loam, silt loam, silt

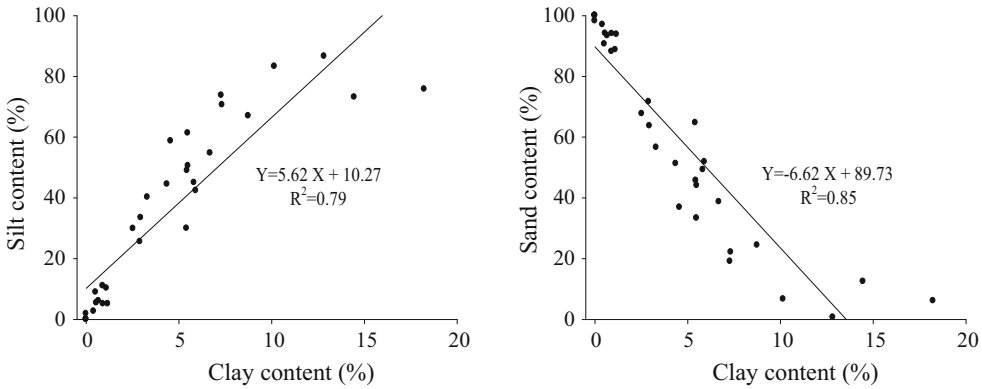

Fig. 7 The relations between clay content and silt/sand content at the 0–10 cm soil depth

fractal dimension of PSD had a highly significant negative correlation with the sand content, and a very significant positive correlation with the clay content, silt content, and soil salinity. A similar study by Millán et al. (2003) on the fractal nature of soils with variation textures showed that the fractal dimension of PSD is significantly positively correlated with clay content following a linear trend.

Conclusion

Excessive salt accumulation in soils is one of the most important global environmental problems especially for arid and semiarid regions. An understanding of vertical and spatial distribution characteristics of soil salinity can help to accurately obtain information about the salinization and

Table 7 Volume fractal dimensions of soil clay, silt and sand

Soil depth (cm)	D	R	D_{Clay}	R_{Clay}	D_{Silt}	R_{Silt}	D_{Sand}	R_{Sand}
0–10	2.553	0.953	2.000	1.000	2.460	0.983	2.609	0.813
10–20	2.555	0.954	2.000	1.000	2.349	0.982	2.595	0.802
20–40	2.503	0.961	2.000	1.000	2.267	0.986	2.569	0.814
40–60	2.543	0.957	2.000	1.000	2.705	0.996	2.578	0.821
60–80	2.524	0.962	2.000	1.000	2.305	0.989	2.554	0.821
80–100	2.509	0.965	2.000	1.000	2.337	0.983	2.512	0.805

D_{Clay}, D_{Silt} and D_{Sand} respectively represent the volume fractal dimension of soil clay, silt and sand, and R_{Clay}, R_{Silt} and R_{Sand} represent the corresponding correlation coefficient

Table 8 Spearman's correlation coefficients from analysis of the associations between soil ions/salinity and soil texture in the study area

Soil depth (cm)	Content (g/L)	Clay (%)		Silt (%)		Sand (%)	
		R	Sig.	R	Sig.	R	Sig.
0–10	CO_3^{2-}	0.298	0.097	0.227	0.212	0.226	0.214
	HCO_3^-	0.008	0.965	0.137	0.454	−0.137	0.455
	Cl^-	0.239	0.187	0.251	0.165	−0.257	0.156
	SO_4^{2-}	0.365*	0.040	0.377*	0.034	−0.386*	0.029
	Ca^{2+}	0.346	0.052	0.338	0.059	−0.345	0.053
	Mg^{2+}	0.281	0.120	0.305	0.090	−0.319	0.075
	$Na^+ + K^+$	0.243	0.181	0.258	0.154	−0.264	0.145
	TDS	0.343	0.055	0.349*	0.050	−0.358*	0.044
10–20	CO_3^{2-}	−0.137	0.447	−0.021	0.907	0.037	0.836
	HCO_3^-	0.179	0.320	0.488**	0.004	−0.455**	0.008
	Cl^-	0.331	0.060	0.472**	0.006	−0.462**	0.007
	SO_4^{2-}	0.105	0.561	0.445**	0.009	−0.407**	0.019
	Ca^{2+}	0.161	0.372	0.415*	0.016	−0.388*	0.026
	Mg^{2+}	0.184	0.306	0.460**	0.007	−0.431*	0.012
	$Na^+ + K^+$	0.135	0.455	0.464**	0.006	−0.428*	0.013
	TDS	0.147	0.413	0.473**	0.005	−0.437**	0.011
20–40	CO_3^{2-}	−0.155	0.390	−0.130	0.472	0.147	0.413
	HCO_3^-	0.607**	0.000	0.574**	0.000	−0.594**	0.000
	Cl^-	0.312	0.077	0.335	0.057	−0.323	0.067
	SO_4^{2-}	0.324	0.066	0.332	0.059	−0.320	0.069
	Ca^{2+}	0.042	0.815	0.010	0.958	−0.007	0.969
	Mg^{2+}	0.391*	0.024	0.407*	0.019	−0.406*	0.019
	$Na^+ + K^+$	0.443**	0.010	0.450**	0.009	−0.442*	0.010
	TDS	0.330	0.061	0.335	0.057	−0.323	0.067
40–60	CO_3^{2-}	−0.101	0.568	−0.094	0.597	0.115	0.518
	HCO_3^-	0.459**	0.006	0.461**	0.006	−0.463**	0.006
	Cl^-	0.191	0.279	0.304	0.081	−0.278	0.112
	SO_4^{2-}	0.277	0.112	0.364*	0.034	−0.356*	0.039
	Ca^{2+}	0.146	0.409	−0.147	0.407	0.142	0.422
	Mg^{2+}	0.283	0.104	0.346*	0.045	−0.353*	0.040
	$Na^+ + K^+$	0.330	0.057	0.428*	0.011	−0.381*	0.016
	TDS	0.300	0.085	0.394*	0.021	−0.965**	0.026
60–80	CO_3^{2-}	−0.133	0.460	−0.125	0.487	0.119	0.511
	HCO_3^-	0.575**	0.000	0.604**	0.000	−0.610**	0.000
	Cl^-	0.405*	0.019	0.381*	0.029	−0.376*	0.031
	SO_4^{2-}	0.483**	0.004	0.439*	0.011	−0.435*	0.011
	Ca^{2+}	0.008	0.964	0.059	0.744	0.063	0.726
	Mg^{2+}	0.576**	0.000	0.507**	0.003	−0.519**	0.002

Table 8 continued

Soil depth (cm)	Content (g/L)	Clay (%)		Silt (%)		Sand (%)	
		R	Sig.	*R*	Sig.	*R*	Sig.
	$Na^+ + K^+$	0.542**	0.001	0.521**	0.002	−0.517**	0.002
	TDS	0.510**	0.002	0.469**	0.006	−0.464**	0.007
80–100	CO_3^{2-}	−0.088	0.619	−0.105	0.555	0.091	0.555
	HCO_3^-	0.412*	0.015	0.420*	0.013	−0.430*	0.013
	Cl^-	0.543**	0.001	0.532**	0.001	−0.529**	0.001
	SO_4^{2-}	0.576**	0.000	0.583**	0.604	−0.580**	0.000
	Ca^{2+}	0.113	0.523	0.092	0.000	−0.086	0.604
	Mg^{2+}	0.596**	0.000	0.589**	0.000	−0.588**	0.000
	$Na^+ + K^+$	0.672**	0.000	0.679**	0.000	−0.675**	0.000
	TDS	0.648**	0.000	0.640**	0.000	−0.637**	0.000

* Correlation is significant at the 0.05 level (2-tailed)

** Correlation is significant at the 0.01 level (2-tailed)

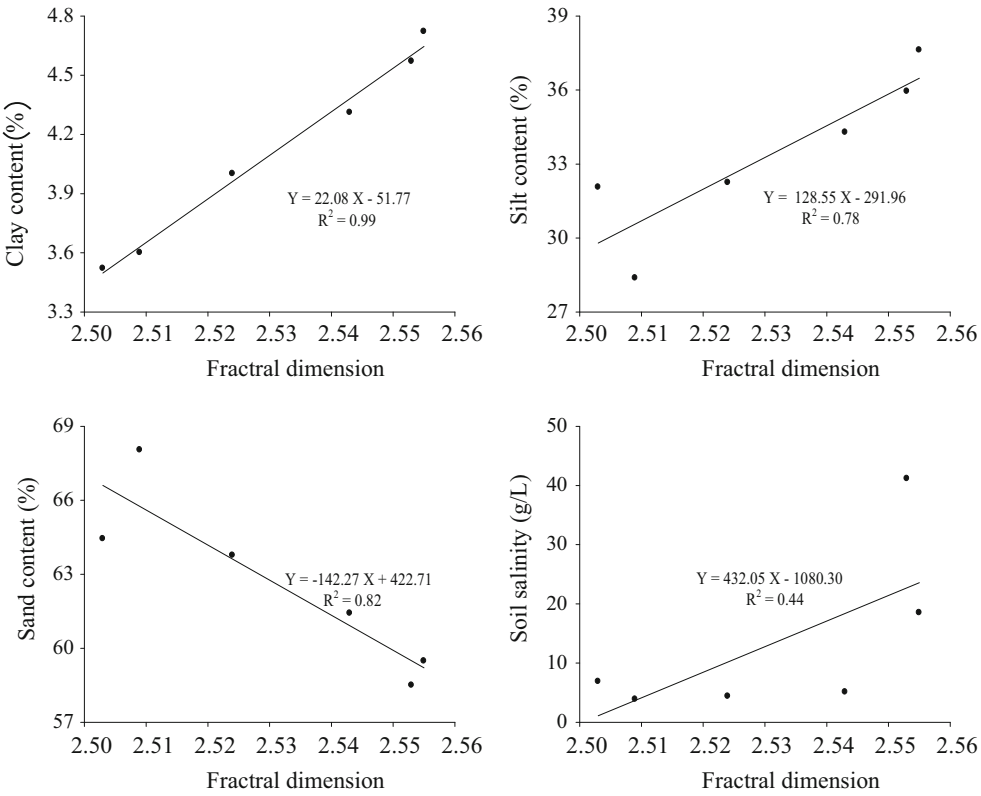

Fig. 8 Relationship between fractal dimension of PSD and clay, silt, sand content, and soil salinity

potential salinization of river system. Using a series of data from the study area, the vertical and spatial variations in soil salinity and soil ions were analyzed using multiple methods.

Based on the ratio of Cl^-/SO_4^{2-}, the main salt types of soil are chloride–sulfate and sulfate in different soil depths in the lower reaches of Heihe River. In the study area, moderate salinized soil, heavy salinized soil and saline soil accounted for 5.71, 25.71, and 42.87 %, respectively. It was shown that soil salinization in the study area is severe. These results have important implications for land resources management in the lower reaches of Heihe River. Given the alarming rates of soil salinization, the amelioration options for saline soil are important for sustainable utilization of land resources. The first point of action must be the leaching of salts from upper to lower soil depths.

Different soil textures and their combination in the soil vertical profile play an important role in governing the changes in soil salinity. Concentration of salt in soil

increases with the decrease of soil particle size. This is because fine particles have high specific area that retains high amounts of salts. The correlation coefficients between soil ions/salinity and soil texture presented in the study area provided a base for understanding of soil texture impacts on concentration of soil ions and soil salinity. These results would be beneficial for the regional planners and policy makers to estimate the changes of soil salinity when soil texture changes over time.

Acknowledgments This research was supported by the Cooperation-Innovation team project of the Chinese Academy of Sciences. The authors are grateful to the reviewers for their helpful comments and suggestions to improve the manuscript.

References

Abdelfattah MA, Shahid SA, Othman YR (2009) Soil salinity mapping model developed using RS and GIS—a case study from Abu Dhabi, United Arab Emirates. Eur J Sci Res 26:342–351

Acosta JA, Cano AF, Arocena JM, Debela F, Martínez-Martínez S (2009) Distribution of metals in soil particle size fractions and its implication to risk assessment of playgrounds in Murcia City (Spain). Geoderma 149:101–109. doi:10.1016/j.geoderma.2008.11.034

Al-Rajahi A, Al-Shayeb SM, Seaward MRD, Edwardst HGM (1996) Particle size effect for metal pollution analysis of atmospherically deposited dust. Atmos Environ 30:145–153

Braak CJFT, Verdonschot PFM (1995) Canonical correspondence analysis and related multivariate methods in aquatic ecology. Aquat Sci 57:256–290

Carter LM, Rhoades JD, Chesson JH (1993) Mechanization of soil salinity assessment for mapping. Paper presented at water meeting of American society of agricultural engineering, Chicago, IL

Cebas-Csic JÁR, Hernández J, Silla RO, Alcaraz F (1997) Patterns of spatial and temporal variations in soil salinity: example of a salt marsh in a semiarid climate. Arid Soil Res Rehabil 11:315–329. doi:10.1080/15324989709381485

Chen XH, Duan ZH, Luo TF (2014) Changes in soil quality in the critical area of desertification surrounding the Ejina Oasis, Northern China. Environ Earth Sci 72:2643–2654. doi:10.1007/s12665-014-3171-3

Chi CM, Wang ZC (2010) Characterizing salt-affected soils of Songnen Plain using saturated paste and 1:5 soil-to-water extraction methods. Arid Land Res Manag 24:1–11. doi:10.1080/15324980903439362

Corwin DL, Lesch SM, Oster JD, Kaffka SR (2006) Monitoring management-induced spatio-temporal changes in soil quality through soil sampling directed by apparent electrical conductivity. Geoderma 131:369–387. doi:10.1016/j.geoderma.2005.03.014

Cunningham MA, Snyder E, Yonkin D, Ross M, Elsen T (2007) Accumulation of deicing salts in soils in an urban environment. Urban Ecosyst 11:17–31. doi:10.1007/s11252-007-0031-x

Deng HM, Jilili A, Ge YX (2013) Analysis on the characteristics of dry lakebed sedimentary soil in Ebinur, Xinjiang Uygur autonomous region. Res Soil Water Conserv 20:14–19 **(In Chinese with English Abstract)**

Fang HL, Liu GH, Kearney M (2005) Georelational analysis of soil type, soil salt content, landform, and land use in the Yellow River Delta, China. Environ Manag 35:72–83. doi:10.1007/s00267-004-3066-2

Feng Q, Si JH, Xi HY, Yu TF, Zhang FP (2015) Ecological water demand and quantity regulation in the lower reaches of Heihe River. Science Press, Beijing **(In Chinese)**

Filgueira RR, Fournier LL, Cerisola CI, Gelati P, García MG (2006) Particle-size distribution in soils: a critical study of the fractal model validation. Geoderma 134:327–334. doi:10.1016/j.geoderma.2006.03.008

Flowers TJ (2004) Improving crop salt tolerance. J Exp Bot 55:307–319

Fu H, Pei SF, Wan CG, Sosebee RE (2009) Fractal dimension of soil particle size distribution along an altitudinal gradient in the Alxa Rangeland, western Inner Mongolia. Arid Land Res Manag 23:137–151. doi:10.1080/15324980902813658

Gao JZ, Su YH, Xi HY, Yu TF (2012) Studies on soil nutrient and salinity along the lower reaches area of Heihe River in arid regions, Northwest of China. J Soil Water Conversat 26:94–99 **(In Chinese with English Abstract)**

Gu FX, Zhang YD, Chu Y, Shi QD (2002) Primary analysis on groundwater, soil moisture and salinity in Fukang Oasis of southern Junggar Basin. Chin Geogr Sci 12:333–338

Guo QL, Feng Q, Li JL (2009) Environmental changes after ecological water conveyance in the lower reaches of Heihe River, Northwest China. Environ Geol 58:1387–1396. doi:10.1007/s00254-008-1641-1

Halmurat G, Abdusalarn J, Hemit Y, Rabiya T (2008) Study on the dynamic characteristics of salt content of salinized soil on Yutian Oasis in Xingjiang autonomous region. Res Soil Water Conserv 15:100–106 **(In Chinese with English Abstract)**

He ZB, Zhao WZ (2006) Characterizing the spatial structures of riparian plant communities in the lower reaches of the Heihe River in China using geostatistical techniques. Ecol Res 21:551–559. doi:10.1007/s11284-006-0160-3

Hillel D (1980) Fundamentals of soil physics. Academic Press, New York

Hu HC, Tian FQ, Hu HP (2011) Soil particle size distribution and its relationship with soil water and salt under mulched drip irrigation in Xinjiang of China. Sci China Technol Sci 54:1568–1574. doi:10.1007/s11431-010-4276-x

Huang GH, Zhan WH (2002) Fractal property of soil particle size distribution and its application. Acta Pedol Sin 39:490–497

Jia HY, Peng HC, Niu DL, Wang QJ (2002) Analysis of the effect of biomeasures on discared salkaline land in Chidamu Basin. Acta Agrestic Sin 10:63–68 **(In Chinese with English Abstract)**

Jia YH, Zhao CY, Nan ZR (2008) Spatial feature of soil salinity in groundwater fluctuant region of the lower reaches of the Heihe River. Arid Land Geogr 31:379–388

Jin Z, Dong YS, Qi YC, Liu WG, An ZS (2013) Characterizing variations in soil particle-size distribution along a grass-desert shrub transition in the Ordos Plateau of Inner Mongolia, China. Land Degrad Dev 24:141–146. doi:10.1002/ldr.1112

Kettler TA, Doran JW, Gilbert TL (2001) Simplified method for soil particle-size determination to accompany soil-quality analyses. Soil Sci Soc Am 65:849–852

Kotuby-Amacher J, Koenig R, Kitchen B (1997) Salinity and plant tolerance. Available at: http://extension.usu.edu/publica/agpubs/salini.htm

Lipiec J, Orellana R (1998) The fractal dimension of pore distribution patterns in variously-compacted soil. Soil Tillage Res 47:61–66

Liu W, Wang T, Su YH, Feng Q (2005) Analysis of the characteristics of soil and groundwater salinity in the lower reaches of Heihe River. J Glaciol Geocryol 27:890–898 **(In Chinese with English Abstract)**

Liu W, Wang ZJ, Xi HY (2008) Variations of physical and chemical properties of water and soil and their siginficance to ecosystem in the lower reaches of Heihe River. J Glaciol Geocryol 30:88–96 **(In Chinese with English Abstract)**

Ljung K, Selinus O, Otabbong E, Berglund M (2006) Metal and arsenic distribution in soil particle sizes relevant to soil ingestion by children. Appl Geochem 21:1613–1624. doi:10.1016/j.apgeochem.2006.05.005

Martin MA, Montero E (2002) Laser diffraction and multifractal analysis for the characterization of dry soil volume-size distributions. Soil Tillage Res 64:113–123

Millan H, Orellana P (2001) Mass fractal dimensions of soil aggregates from different depths of a compacted. Vertisol For Soil Anal Methods 101:65–76

Millán M, González-Posada M, Aguilar M, Domínguez J, Céspedes L (2003) On the fractal scaling of soil data. Particle-size distributions. Geoderma 117:117–128

Montero ES (2005) Rényi dimensions analysis of soil particle-size distributions. Ecol Model 182:305–315. doi:10.1016/j.ecolmodel.2004.04.007

Nawar S, Buddenbaum H, Hill J (2015) Estimation of soil salinity using three quantitative methods based on visible and near-infrared reflectance spectroscopy: a case study from Egypt. Arab J Geosci 8:5127–5140. doi:10.1007/s12517-014-1580-y

Qadir M, Ghafoor A, Murtaza G (2000) Amelioration strategies for saline soils—a review. Land Degrad Dev 11:501–521

Rengasamy P (2006) World salinization with emphasis on Australia. J Exp Bot 57:1017–1023. doi:10.1093/jxb/erj108

Rogel JA, Ariza FA, Silla RO (2000) Soil salinity and moisture gradients and plant zonation in Mediterranean salt marshes of Southeast Spain. Wetlands 20:357–372

Su YZ, Zhao HL, Zhao WZ, Zhang TH (2004) Fractal features of soil particle size distribution and the implication for indicating desertification. Geoderma 122:43–49. doi:10.1016/j.geoderma.2003.12.003

Su YH, Feng Q, Zhu GF, Si JH, Zhang YW (2007) Identification and evolution of groundwater chemistry in the Ejin Sub-Basin of the Heihe River, Northwest China. Pedosphere 17:331–342. doi:10.1016/s1002-0160(07)60040-x

Su YH, Zhu GF, Feng Q, Li ZZ, Zhang FP (2008) Environmental isotopic and hydrochemical study of groundwater in the Ejina Basin, Northwest China. Environ Geol 58:601–614. doi:10.1007/s00254-008-1534-3

Tyler SW, Wheatcraft SW (1992) Fractal scaling of soil particle-size distributions-analysis and liminations. Soil Sci Soc Am 56:362–369

Wang SQ, Zhu SL, Zhou CH (2001) Characteristics of spatial variability of soil thickness in China. Geogr Res 20:161–167

Wang GL, Zhou SL, Zhao QG (2005) Volume fractal dimension of soil particles and its application to land use. Acta Ecol Sin 42:547–550 **(In Chinese with English Abstract)**

Wang YG, Li Y, Xiao DN (2008) Catchment scale spatial variability of soil salt content in agricultural oasis, Northwest China. Environ Geol 56:439–446. doi:10.1007/s00254-007-1181-0

Wang YG, Zheng XJ, Li Y (2009) Change characteristics of soil salt content in different landscape units in arid region. Chin J Ecol 28:2293–2298

Wen XH, Wu Y, Su J, Zhang Y, Liu F (2005) Hydrochemical characteristics and salinity of groundwater in the Ejina Basin, Northwestern China. Environ Geol 48:665–675. doi:10.1007/s00254-005-0001-7

Wu WY, Yin SY, Liu HL, Niu Y, Bao Z (2014) The geostatistic-based spatial distribution variations of soil salts under long-term wastewater irrigation. Environ Monit Assess 186:6747–6756. doi:10.1007/s10661-014-3886-3

Xi HY, Feng Q, Si JH, Chang ZQ, Cao SK (2009) Impacts of river recharge on groundwater level and hydrochemistry in the lower reaches of Heihe River Watershed, northwestern China. Hydrogeol J 18:791–801. doi:10.1007/s10040-009-0562-8

Yang M, Yanful EK (2002) Water balance during evaporation and drainage in cover soils under different water table conditions. Adv Environ Res 6:505–521

Yang PL, Luo YP, Shi YC (1993) Soil fractal characteristics measured by mass of particle-size distribution. Chin Sci Bull 38:1896–1899 **(In Chinese with English Abstract)**

Yi LP, Ma J, Li Y (2007) Soil salt and nutrient concentration in the rhizosphere of desert halophytes. Acta Ecol Sin 29:3565–3571 **(In Chinese with English Abstract)**

Yidana SM, Yidana A (2010) An assessment of the origin and variation of groundwater salinity in southeastern. Ghana Environ Earth Sci 61:1259–1273. doi:10.1007/s12665-010-0449-y

Yu TR, Wang ZQ (1988) Soil chemical analysis. Chinese Science Press, Beijing **(In Chinese)**

Yu TF, Feng Q, Liu W, Si JH, Xi HY, Chen LJ (2012) Soil water and salinity in response to water deliveries and the relationship with plant at the lower reaches of Heihe River. Acta Ecol Sin 32:7009–7017 **(In Chinese with English Abstract)**

Yu JB et al (2013) The spatial distribution characteristics of soil salinity in coastal zone of the Yellow River Delta. Environ Earth Sci 72:589–599. doi:10.1007/s12665-013-2980-0

Zhang DF, Wang SJ (2001) Mechanism of freeze–thaw action in the process of soil salinization in northeast China. Environ Geol 41:96–100

Zhang XY, Gong JD, Zhou MX (2004) Analysis on characters of soil salinity in Ejin Delta. J Desert Res 24:442–447 **(In Chinese with English Abstract)**

Zhang LP, Zhang YL, Wang AY (2006) Automatic soil texture classification system based on computer graphics. Prog Geogr 25:86–95 **(In Chinese with English Abstract)**

Zhang TJ, Yang JS, Liu GM, Yang QY (2010) Application of grey system theory evaluating the influencing factors of soil salinity. Chin J Soil Sci 41:793–796

Zhang TT, Zeng SL, Gao Y, Ouyang ZT, Li B, Fang CM, Zhao B (2011) Assessing impact of land uses on land salinization in the Yellow River Delta, China using an integrated and spatial statistical model. Land Use Policy 28:857–866. doi:10.1016/j.landusepol.2011.03.002

Zhao XF, Yang JS, Yao RJ (2010) Characteristics of soil salinization in mudflat of north Jiangsu province based on canonical correspondence analysis. Acta Pedol Sin 47:422–428 **(In Chinese with English Abstract)**

Zhong HP, Liu H, Wang Y, Tuo Y, Geng LH, Yan ZJ (2002) Relationship between Ejina oasis and water resources in the lower Heihe River basin. Adv Water Sci 13:223–228 **(In Chinese with English Abstract)**

Zhou X, Fang B, Wan L, Cao WB, Wu SJ, Feng WD (2006) Occurrence of soluble salts and moisture in the unsaturated zone and groundwater hydrochemistry along the middle and lower reaches of the Heihe River in northwest China. Environ Geol 50:1085–1093. doi:10.1007/s00254-006-0282-5

Zhu GF, Su YH, Huang CL, Feng Q, Liu ZG (2009) Hydrogeochemical processes in the groundwater environment of Heihe River Basin, Northwest China. Environ Earth Sci 60:139–153. doi:10.1007/s12665-009-0175-5